

# Supplementary material:

## Ampere-Oersted field splitting of the nonlinear spin-torque vortex oscillator dynamics

Flavio ABREU ARAUJO<sup>1,\*</sup>, Chloé CHOPIN<sup>1</sup>, and Simon de WERGIFOSSE<sup>1</sup>

<sup>1</sup>Institute of Condensed Matter and Nanosciences, Université catholique de Louvain, Place Croix du Sud 1, 1348 Louvain-la-Neuve, Belgium

\*flavio.abreuaraujo@uclouvain.be

### The harmonic oscillator equation

Our oscillator dynamics is described the following homogeneous system of linear first-order differential equations:

$$\dot{\mathbf{X}} = \bar{\bar{\Omega}}\mathbf{X} \quad (1)$$

where the matrix  $\bar{\bar{\Omega}}$  is given as:

$$\bar{\bar{\Omega}} = \begin{bmatrix} \Gamma & -\omega \\ \omega & \Gamma \end{bmatrix} \quad (2)$$

Considering  $\Gamma$  and  $\omega$  as being constant one can derive time-dependent solutions for the vortex core position  $(X(t), Y(t))$ . This assumption is verified in a steady-state regime of oscillation. The eigenvalues  $\lambda$  of the system are calculated from its characteristic equation:

$$\lambda^2 - 2\Gamma\lambda + (\Gamma^2 + \omega^2) = 0 \quad (3)$$

The latter has been obtained from  $\det(\bar{\bar{\Omega}} - \lambda\bar{\bar{\mathbf{I}}}) = 0$ . The two solutions of Eq. (3) are  $\lambda = \Gamma \pm i\omega$ . Using Euler's formula one can prove that the coordinates of the vortex core are given as:

$$X(t) = e^{\Gamma t}[(C_1 + C_2)\cos(\omega t) + i(C_1 - C_2)\sin(\omega t)]$$

$$Y(t) = e^{\Gamma t}[-i(C_1 - C_2)\cos(\omega t) + (C_1 + C_2)\sin(\omega t)]$$

If the two constants are fixed such as  $C_1 = -C_2 = -\frac{i}{2}\|\mathbf{X}\|$  one finally obtains:

$$\begin{bmatrix} X(t) \\ Y(t) \end{bmatrix} = \|\mathbf{X}\|e^{\Gamma t} \begin{bmatrix} \sin(\omega t) \\ -\cos(\omega t) \end{bmatrix} \quad (4)$$

### Ampère-Oersted field contribution to the Thiele equation

Ampère's law (SI):

$$\begin{aligned} \oint_c \mathbf{B} \cdot d\ell &= 4\pi k_m I_c \\ &= \mu_0 I_c \end{aligned}$$

where  $k_m$  is the magnetic force constant ( $\mu_0/(4\pi)$ ) and  $\mu_0$  is the magnetic constant [ $(4\pi \cdot 10^{-7} \text{ T/(A/m)}$ ].

Let's take the case of an infinite wire of radius  $R$  with a uniform current  $I$  flowing through it.  $I_c$  represents the current flowing inside the path  $c$  of integration.

Inside the wire ( $r \leq R$ ):  $I_c = I\pi r^2/(\pi R^2) = Ir^2/R^2 = \pi J r^2$ , where  $J = I/(\pi R^2)$  is the current density. Outside the wire ( $r > R$ ):  $I_c = I$ .

$$\Rightarrow \oint_c \mathbf{B} \cdot d\ell = B2\pi r = \mu_0 I_c$$

For  $r \leq R$  (inside the wire):  $B2\pi r = \mu_0\pi|J|r^2$  and  $B(r) = \frac{\mu_0|J|}{2}r$

For  $r > R$  (outside the wire):  $B2\pi r = \mu_0\pi R^2|J|$  and  $B(r) = \frac{\mu_0|J|}{2}R^2\frac{1}{r}$

The Oersted field vector obtained is:  $\mathbf{B}(\mathbf{r}) = B(r) (\cos(\theta + \sigma\frac{\pi}{2}), \sin(\theta + \sigma\frac{\pi}{2}), 0) = B(r)\mathbf{b}(\mathbf{r})$ , where  $\mathbf{r} = r(\cos\theta, \sin\theta, 0)$  or  $\mathbf{r} = (r, \theta)$ ,  $\sigma = \text{sign}(J) = \pm 1$  and  $\mathbf{b}(\mathbf{r})$  is the Oersted field unit vector. Inside a magnetic dot of radius  $R$  and thickness  $h$ , the potential energy due to the current induced Oersted field and a shifted magnetic vortex state of magnetization distribution  $\mathbf{M}(\mathbf{r}, \mathbf{X})$  with  $\mathbf{X} = (\rho, \varphi)$  being the vortex core position is given by:

$$W_{\text{Oe}} = - \int_V \mathbf{B}(\mathbf{r}) \cdot \mathbf{M}(\mathbf{r}, \mathbf{X}) dV,$$

where  $V$  corresponds to the magnetic dot volume.

In SI units  $B_{\text{SI}}(r) = \frac{\mu_0|J|}{2}r = Q_{\text{SI}}|J|r$  [T], with  $Q_{\text{SI}} = \frac{\mu_0}{2}$  [T·m/A], and  $J \Rightarrow [A/m^2]$ .

In CGS units  $B_{\text{CGS}}(r) = \frac{\pi|J|}{5}r = Q_{\text{CGS}}|J|r$  [G], with  $Q_{\text{CGS}} = \frac{\pi}{5}$  [G·cm/A], and  $J \Rightarrow [A/cm^2]$ .

$\mathbf{B}(\mathbf{r}) = B(r)\mathbf{b}(\mathbf{r}) = Q|J|r\mathbf{b}(\mathbf{r})$  and  $\mathbf{M}(\mathbf{r}, \mathbf{X}) = M_s\mathbf{m}(\mathbf{r}, \mathbf{X})$ , where  $M_s$  is the spontaneous magnetisation and  $\mathbf{m}(\mathbf{r}, \mathbf{X})$  is the normalised magnetisation profile (distribution) of the magnetic vortex. The potential energy  $W_{\text{Oe}}$  yields:

$$W_{\text{Oe}} = -Q|J|M_s \int_V r\mathbf{b}(\mathbf{r}) \cdot \mathbf{m}(\mathbf{r}, \mathbf{X}) dV.$$

As  $\mathbf{b}(\mathbf{r}) = (\cos\phi_1, \sin\phi_1, 0)$ , with  $\phi_1 = \theta + \sigma\pi/2$ , has no out of plane component, the  $z$ -component (vortex core shape) of  $\mathbf{m}(\mathbf{r}, \mathbf{X})$  is not contributing, so  $\Rightarrow \mathbf{m} = (\cos\phi_2, \sin\phi_2, 0)$ , i.e.  $\Rightarrow \mathbf{m}(\mathbf{r}, \mathbf{X}) = (\cos[\phi_2(\mathbf{r}, \mathbf{X})], \sin[\phi_2(\mathbf{r}, \mathbf{X})], 0)$ .

The in-plane profile  $\phi_2(\mathbf{r}, \mathbf{X})$  of an off-centred vortex is well described within the "Two Vortex Ansatz" TVA (or "Image Vortex Ansatz", IVA) as no side charges are created (unlike the "Single Vortex Ansatz" also called the "Rigid Vortex Ansatz"):

$$\phi_2^{\text{TVA}}(\mathbf{r}, \mathbf{X}) = \arg(\mathbf{r} - \mathbf{X}) + \arg(\mathbf{r} - \mathbf{X}_I) - \varphi + C\pi/2$$

where  $\mathbf{X}_I = (R^2/\rho, \varphi)$  are the image vortex coordinates ( $\|\mathbf{X}_I\| = R^2/\rho^2 \|\mathbf{X}\|$ ) and  $C$  is the vortex chirality ( $= \pm 1$ ).

One obtains explicitly:

$$\phi_2^{\text{TVA}}(\mathbf{r}, \mathbf{X}) = \tan^{-1} \left( \frac{r \sin \theta - \rho \sin \varphi}{r \cos \theta - \rho \cos \varphi} \right) + \tan^{-1} \left( \frac{\rho r \sin \theta - R^2 \sin \varphi}{\rho r \cos \theta - R^2 \cos \varphi} \right) - \varphi + C\frac{\pi}{2}$$

The cylindrical symmetry of the energy evaluation of an off-centred vortex with respect to the Oersted field makes it independent from  $\varphi$ , so we choose to take  $\varphi = 0$ :

$$\phi_2^{\text{TVA}}(r, \rho, \theta) = \tan^{-1} \left( \frac{r \sin \theta}{r \cos \theta - \rho} \right) + \tan^{-1} \left( \frac{\rho r \sin \theta}{\rho r \cos \theta - R^2} \right) + C\frac{\pi}{2}$$

Finally, using reduced variables  $\eta = r/R$  and  $s = \rho/R$  we obtain:

$$\phi_2^{\text{TVA}}(\eta, s, \theta) = \tan^{-1} \left( \frac{\eta \sin \theta}{\eta \cos \theta - s} \right) + \tan^{-1} \left( \frac{s \eta \sin \theta}{s \eta \cos \theta - 1} \right) + C\frac{\pi}{2}$$

$$\begin{aligned} W_{\text{Oe}} &= -Q|J|M_s \int_V r\mathbf{b}(\mathbf{r}) \cdot \mathbf{m}(\mathbf{r}, \mathbf{X}) dV \\ &= -Q|J|M_s \int_0^R \int_0^{2\pi} \int_0^h r^2 \mathbf{b}(\mathbf{r}) \cdot \mathbf{m}(\mathbf{r}, \mathbf{X}) dr d\theta dz \\ &= -Q|J|M_s h \int_0^R \int_0^{2\pi} r^2 \mathbf{b}(\mathbf{r}) \cdot \mathbf{m}(\mathbf{r}, \mathbf{X}) dr d\theta \end{aligned}$$

The previous transformation is due to the fact that there is no  $z$ -dependence.

As  $\eta = r/R$ ,  $dr = R d\eta$ :

$$\begin{aligned} W_{\text{Oe}} &= -Q|J|M_s h \int_0^1 \int_0^{2\pi} R^2 \frac{r^2}{R^2} \mathbf{b}(\mathbf{r}) \cdot \mathbf{m}(\mathbf{r}, \mathbf{X}) R d\eta d\theta \\ &= -Q|J|M_s h R^3 \int_0^1 \int_0^{2\pi} \eta^2 \mathbf{b}(\mathbf{r}) \cdot \mathbf{m}(\mathbf{r}, \mathbf{X}) d\eta d\theta \end{aligned}$$

$$\begin{aligned} \mathbf{b}(\mathbf{r}) \cdot \mathbf{m}(\mathbf{r}, \mathbf{X}) &= (\cos \phi_1, \sin \phi_1, 0) \cdot (\cos \phi_2^{\text{TVA}}, \sin \phi_2^{\text{TVA}}, 0) \\ &= \cos \phi_1 \cos \phi_2^{\text{TVA}} + \sin \phi_1 \sin \phi_2^{\text{TVA}} \\ &= \cos(\phi_1 - \phi_2^{\text{TVA}}) \end{aligned}$$

$$\begin{aligned} \phi_1 - \phi_2^{\text{TVA}} &= \theta + \sigma \frac{\pi}{2} - \tan^{-1} \left( \frac{\eta \sin \theta}{\eta \cos \theta - s} \right) - \tan^{-1} \left( \frac{s\eta \sin \theta}{s\eta \cos \theta - 1} \right) - C \frac{\pi}{2} \\ &= \theta + (\sigma - C) \frac{\pi}{2} - \tan^{-1} \left( \frac{\eta \sin \theta}{\eta \cos \theta - s} \right) - \tan^{-1} \left( \frac{s\eta \sin \theta}{s\eta \cos \theta - 1} \right) \end{aligned}$$

Using  $\theta = \tan^{-1} \left( \frac{\sin \theta}{\cos \theta} \right)$  and  $\tan^{-1}(a) \pm \tan^{-1}(b) = \tan^{-1} \left( \frac{a \pm b}{1 \mp ab} \right)$ :

$$\begin{aligned} \phi_1 - \phi_2^{\text{TVA}} &= (\sigma - C) \frac{\pi}{2} + \tan^{-1} \underbrace{\left( \frac{\sin \theta}{\cos \theta} \right)}_{\lambda} - \tan^{-1} \underbrace{\left( \frac{s\eta^2 \sin 2\theta - \eta(1+s^2) \sin \theta}{s\eta^2 \cos 2\theta - \eta(1+s^2) \cos \theta + s} \right)}_{\mu} \\ &= (\sigma - C) \frac{\pi}{2} + \tan^{-1} \left( \frac{\lambda - \mu}{1 + \lambda \mu} \right) \end{aligned}$$

$$\begin{aligned} \mathbf{b}(\mathbf{r}) \cdot \mathbf{m}(\mathbf{r}, \mathbf{X}) &= \cos \left[ \underbrace{(\sigma - C) \frac{\pi}{2}}_A + \underbrace{\tan^{-1} \left( \frac{\lambda - \mu}{1 + \lambda \mu} \right)}_B \right] \\ &= \cos A \cos B - \underbrace{\sin A \sin B}_{= 0 \text{ (} A = 0 \text{ or } \pi \text{)}} \\ &= \cos \left( (\sigma - C) \frac{\pi}{2} \right) \cos \left( \tan^{-1} \left( \frac{\lambda - \mu}{1 + \lambda \mu} \right) \right) \\ &= \sigma C \frac{1}{\sqrt{1 + \left( \frac{\lambda - \mu}{1 + \lambda \mu} \right)^2}} \end{aligned}$$

$$\mathbf{b}(\mathbf{r}) \cdot \mathbf{m}(\mathbf{r}, \mathbf{X}) = \sigma C \frac{\eta (s^2 + 1) - s \cos(\theta) (\eta^2 + 1)}{\sqrt{(\eta (s^2 + 1) - s \cos(\theta) (\eta^2 + 1))^2 + s^2 \sin(\theta)^2 (\eta^2 - 1)^2}}$$

Finally, the potential energy writes ( $\sigma|J| = J$ ):

$$W_{\text{Oe}}(s) = -Q J C M_s h R^3 \int_0^1 \int_0^{2\pi} \Theta(s, \eta, \theta) d\eta d\theta, \quad (5)$$

where

$$\Theta(s, \eta, \theta) = \frac{\eta^3 (s^2 + 1) - \eta^2 s \cos(\theta) (\eta^2 + 1)}{\sqrt{(\eta (s^2 + 1) - s \cos(\theta) (\eta^2 + 1))^2 + s^2 \sin^2(\theta) (\eta^2 - 1)^2}}.$$

There are two possibilities to evaluate Eq. (5) to obtain the  $s = \rho/R$  dependence of  $W_{\text{Oe}}$ . The first is to numerically integrate it and then to fit the result to a power law in  $s$ . The second possibility is to compute the Taylor expansion (TE) of the integrand of Eq. (5) and then solve it analytically. Both techniques are considered and compared hereafter. Figure S1 shows the numerical resolution of the integral in Eq. (5) in blue. The order 6 power law fit is plotted in red and the order 2, 4, and 10 Taylor expansions are represented with dashed lines.

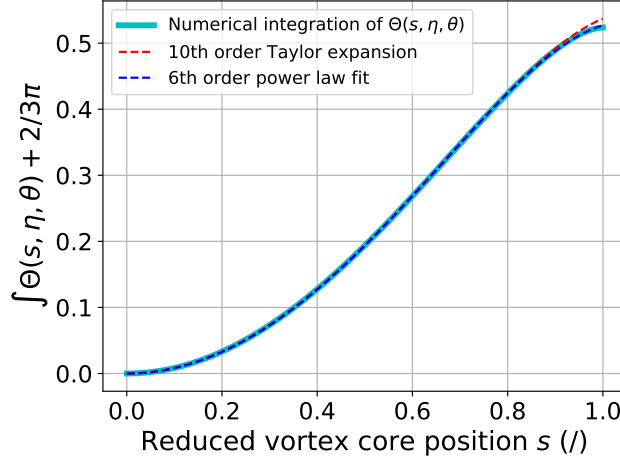


**Figure S1.** Evolution of the double integral in Eq. (5) vs. reduced vortex core position  $s$ . The thick light blue line corresponds to the numerical integration, the dashed blue line is the  $6^{\text{th}}$  order fit over the numerical data and the dashed red line is the results after analytical integration of the  $10^{\text{th}}$  order Taylor expansion.

It should be noticed that  $2/3\pi$  has been added to the overall value of the integral shown in Fig. S1 in such a way to start at 0 and avoid the evaluation of this parameter during the fit. The fitting coefficients are given as follow:

$$W_{\text{Oe}}^{\text{fit}}(s) = -QJCM_s hR^3 \left( -\frac{2}{3}\pi + 0.827s^2 - 0.180s^4 - 0.119s^6 \right). \quad (6)$$

The  $10^{\text{th}}$  order Taylor expansion gives:

$$W_{\text{Oe}}^{\text{TE}}(s) = -QJCM_s hR^3 \left( -\frac{2}{3}\pi + \frac{4\pi}{15}s^2 - \frac{8\pi}{105}s^4 - \frac{4\pi}{315}s^6 - \frac{16\pi}{3465}s^8 - \frac{20\pi}{9009}s^{10} \right). \quad (7)$$

Figure S2 shows the error level between the numerical integration data and both, the fit [Eq. (6)] and the 10th order Taylor expansion [Eq. (7)].

An important consequence of the error level comparison is the fact that the 10th order TE is much more accurate than the fit for  $s \leq 0.78$ , but for  $s > 0.78$  the fit maintains a lower error level.

As mentioned in the main text of this manuscript, the vortex core is unstable for  $s > 0.8$ , so the Taylor expansion is a better choice for modelling the Ampère-Oersted field contribution to the Thiele equation.

The current induced Oersted field acts as a restoring force and one can thus consider:

$$W_{\text{Oe}}(X) = \frac{1}{2}k_{\text{Oe}}X^2, \quad (8)$$

where  $X$  ( $= \rho$ ) is the vortex core orbital radius and  $k_{\text{Oe}}$  is restoring force constant (also called vortex stiffness parameter). The corresponding restoring force magnitude writes:

$$F_{\text{Oe}}(X) = -\frac{\partial W_{\text{Oe}}(X)}{\partial X} = -k_{\text{Oe}}(X)X. \quad (9)$$

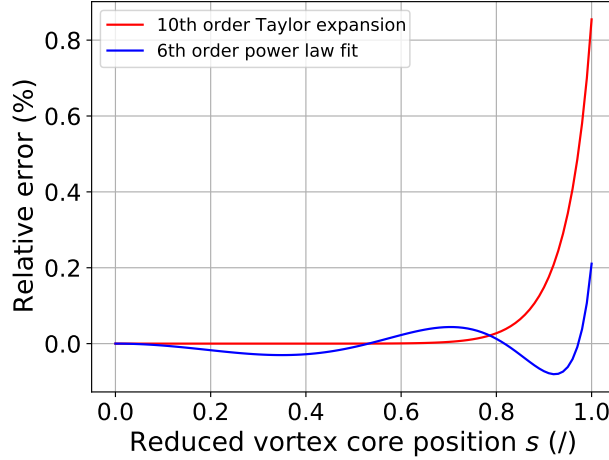


**Figure S2.** Evolution of the relative error level between the numerical integration data and both, the fit [order 6<sup>th</sup> power law, Eq. (6)] and the 10<sup>th</sup> order Taylor expansion [Eq. (7)].

The energy  $W_{\text{Oe}}$  in Eqs. (6) and (7) is already depending on  $s$ , so we can rewrite Eq. (9) as follow to consider the force in terms of the reduced vortex core position  $s$ :

$$\begin{aligned} \frac{F_{\text{Oe}}(s)}{R} &= -\frac{1}{R} \frac{\partial W_{\text{Oe}}(s)}{\partial s} \frac{\partial s}{\partial X} = -k_{\text{Oe}}(s) \frac{X}{R}, \\ &= -\frac{1}{R^2} \frac{\partial W_{\text{Oe}}(s)}{\partial s} = -k_{\text{Oe}}(s)s. \end{aligned}$$

Eqs. (6) and (7) then give the following results for the respective restoring force constants:

$$\begin{aligned} k_{\text{Oe}}^{\text{fit}}(s) &= QJCM_s hR (1.654 - 0.720s^2 - 0.714s^4) \\ &= QJCM_s hR \cdot 1.654 (1 - 0.435s^2 - 0.432s^4), \end{aligned}$$

and

$$\begin{aligned} k_{\text{Oe}}^{\text{TE}}(s) &= QJCM_s hR \left( \frac{8\pi}{15} - \frac{32\pi}{105}s^2 - \frac{24\pi}{315}s^4 - \frac{128\pi}{3465}s^6 - \frac{200\pi}{9009}s^8 \right) \\ &= QJCM_s hR \frac{8\pi}{15} \left( 1 - \frac{4}{7}s^2 - \frac{1}{7}s^4 - \frac{16}{231}s^6 - \frac{125}{3003}s^8 \right). \end{aligned} \quad (10)$$

Finally, the oscillation frequency contribution of the Oersted field is given by  $\omega_{\text{Oe}} = k_{\text{Oe}}/G$ .

$$\omega_{\text{Oe}}^{\text{fit}}(s) = \frac{1.654 \cdot QJCR\gamma_G}{2\pi} (1 - 0.435s^2 - 0.432s^4),$$

and

$$\omega_{\text{Oe}}^{\text{TE}}(s) = \frac{4QJCR\gamma_G}{15} \left( 1 - \frac{4}{7}s^2 - \frac{1}{7}s^4 - \frac{16}{231}s^6 - \frac{125}{3003}s^8 \right).$$

## Magnetostatic contribution to the Thiele equation

The magnetostatic contribution  $W_{\text{ms}}(\xi, s)$  to the Thiele equation has been calculated by Gaididei *et al.*<sup>1</sup> under the "Two Vortex Ansatz" and gives the following equation:

$$W_{\text{ms}}(\xi, s) = \frac{4M_s^2 h^2 R s^2}{\pi} \Theta(\xi, s), \quad (11)$$

with

$$\Theta(\xi, s) = \int_0^1 d\zeta \int_0^1 d\eta \int_0^1 d\eta' \int_0^{2\pi} d\varphi \int_0^{2\pi} d\varphi' \Gamma(\zeta, \eta, \eta', \varphi, \varphi', \xi, s),$$

$$\Gamma(\zeta, \eta, \eta', \varphi, \varphi', \xi, s) = \frac{\eta \eta' (1 - \zeta) \Lambda(\eta, s, \varphi) \Lambda(\eta', s, \varphi + \varphi')}{\sqrt{\eta^2 + \eta'^2 - 2\eta\eta' \cos \varphi' + 4\xi^2 \zeta^2}},$$

and

$$\Lambda(\eta, s, \varphi) = \frac{\eta \sin \varphi}{\sqrt{s^2 + \eta^2 - 2s\eta \cos \varphi} \sqrt{1 + s^2 \eta^2 - 2s\eta \cos \varphi}},$$

where

$$s = \frac{X}{R}, \xi = \frac{h}{2R}, \eta = \frac{r}{R}, \eta' = \frac{r'}{R}.$$

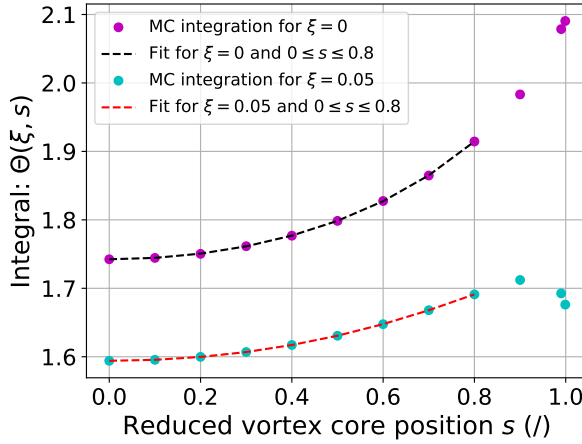


**Figure S3.** Evolution of the integral  $\Theta(\xi, s)$  (see Eq. (11)) vs. the reduced vortex position  $s$ . The magenta dots represent the numerical Monte Carlo integration for  $\xi = 0$  whereas the cyan dots represent the Monte Carlo integration for  $\xi = 0.05$ . The dashed lines correspond to a 6<sup>th</sup> order power law fit of the numerical data in the range of stability of the vortex, i.e.  $0 \leq s \leq 0.8$ . The black and red dashed lines correspond to  $\xi = 0$  and  $\xi = 0.05$ , respectively. The coefficients of the power law model are given in Table S1.

There is no analytical solution for Eq. (11) and a deterministic numerical integration is not feasible. So, we performed a Monte Carlo (MC) integration (non-deterministic) with guaranteed absolute precision of  $10^{-4}$ .<sup>1</sup> It should be noticed that an analytical solution exists when  $\xi = 0$  and  $s = 0$ .<sup>1</sup> obtained  $\Theta(0, 0) = 2\pi(2\mathcal{C} - 1)/3 \simeq 1.742393$  where  $\mathcal{C} = 0.5 \int_0^1 K(x) dx \simeq 0.916$  with  $K(x)$  the elliptic integral of the first kind.

The MC integration for  $\Theta(\xi = 0, s)$  gives after fitting the numerical data to a power law:

$$k_{\text{ms}}^{\xi=0.0}(s) = \frac{8M_s^2 h^2}{R} 1.7424 \left( 1 + 0.1165s^2 - 0.0434s^4 + 0.0243s^6 \right). \quad (12)$$

Even if the practical magnetic dot geometries give rise to very small  $\xi$  values, the latter are not zero. For instance in this manuscript,  $R = 100$  nm and  $h = 10$  nm, so  $\xi = h/(2R) = 0.05$ . The Monte Carlo integration for  $\Theta(\xi = 0.05, s)$ , gives after fit:

$$k_{\text{ms}}^{\xi=0.05}(s) = \frac{8M_s^2 h^2}{R} 1.5941 \left( 1 + 0.0870s^2 + 0.0236s^4 - 0.0171s^6 \right) \quad (13)$$

The mean relative overestimation of Eq. (12) compared to Eq. (13) is about 10.3%. It goes from 9.3% at  $s = 0$  to 13.2% at  $s = 0.8$ . As the oscillation frequency contribution of the magnetostatic energy is given by  $\omega_{\text{ms}} = k_{\text{ms}}/G$ , the vortex core gyroscopic frequencies computed using  $\xi = 0$  instead of  $\xi = 0.05$  in this case give rise to a mean error of about 10.3%.

<sup>1</sup>The library used for the MC integration is GAIL version 2.0 (Guaranteed Automatic Integration Library) developed by the Illinois Institute of Technology.

$\xi$	$\Sigma_0^\xi$	$a^\xi$	$b^\xi$	$c^\xi$
0.0	1.7424	0.1165	0.0434	0.0243
0.05	1.5941	0.0870	0.0236	-0.0171

**Table S1.** Values of the coefficients of the  $k_{\text{ms}}$  term after the fit according to the power law model given in the main text.

## References

1. Gaididei, Y., Kravchuk, V. P. & Sheka, D. D. Magnetic vortex dynamics induced by an electrical current. *Int. J. Quantum Chem.* **110**, 83–97 (2010).